

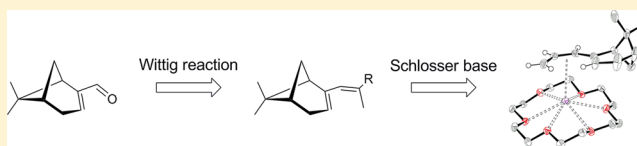
Synthesis and Coordination Chemistry of Pentadienyl Ligands Derived from (1R)-(-)-Myrtenal

Ann Christin Fecker, Bogdan-Florin Crăciun,[†] Matthias Freytag, Peter G. Jones, and Marc D. Walter*

Institut für Anorganische und Analytische Chemie, Technische Universität Braunschweig, Hagenring 30, 38106 Braunschweig, Germany

Supporting Information

ABSTRACT: With the natural product (1R)-(-)-myrtenal as the starting material, a series of chiral pentadienes (PdI*) such as dimethylnopadiene (**2a**), methylphenylnopadiene (**2b**), and methylnopadiene (**2c**) have been prepared by Wittig reactions. Deprotonation with the Schlosser base gives the corresponding potassium pentadienides **3a-K–3c-K**, whose structures were investigated by NMR spectroscopy and X-ray diffraction studies. In all cases a “U” conformation was observed. Furthermore, the coordination chemistry and electronic properties of these new pentadienyl systems were explored in several half-open zirconocene complexes $[(\eta^7\text{-C}_7\text{H}_7)\text{Zr}(\eta^5\text{-PdI}^*)]$ and their PMe_3 and $t\text{BuNC}$ adducts. Density functional theory (DFT) computations are consistent with the experimentally observed face selectivity upon metal coordination: namely, that the metal coordinates exclusively from the sterically less encumbered side.



INTRODUCTION

Cyclopentadienyl (Cp) and its functionalized derivatives are prominent spectator ligands in organometallic chemistry,¹ and their electronic and steric properties are readily modified by simple organic transformations.^{1g,2} Furthermore, enantiomerically pure derivatives have been successfully employed in stereoselective catalytic transformations since 1978.³ At about the same time, Ernst began his investigations on the metal-organic chemistry of pentadienyl (Pdl) ligands, which can be considered as “open” cyclopentadienyl congeners,⁴ and since then a large number of pentadienyl complexes have been prepared. However, in contrast to the plethora of cyclopentadienyl (Cp) ligands, the studies on pentadienyls have mainly focused on C_5H_7 or on alkyl- or trimethylsilyl-substituted derivatives such as 2,4- $\text{Me}_2\text{C}_5\text{H}_5$ and 1,5-(Me_3Si) $_2\text{C}_5\text{H}_5$.⁵ Nevertheless, there are several scattered reports of phenyl-substituted pentadienyl transition-metal complexes,⁶ but the only systematic study, focusing on open and half-open ruthenocenes with phenyl substituents, was reported by Ernst.⁷ Furthermore, several complexes with “edge-bridged” pentadienyl ligands such as cyclooctadienyl⁸ and heteropentadienyl derivatives have been investigated.⁹ From these studies several distinct features of the pentadienyl ligand have emerged. In contrast to the case for Cp, the Pdl framework is able more readily to adopt multiple coordination modes such as η^1 , η^3 , and η^5 and to isomerize between them.^{5,10} In general, η^5 -coordinated pentadienyls form thermally stable complexes, and the larger area enclosed by the five pentadienyl carbon atoms forces the metal atom to approach the pentadienyl plane more closely than it would approach a cyclopentadienyl ring.^{5d} Overall, this stronger interaction between the pentadienyl ligand combined with a shorter metal–pentadienyl separation might mediate enhanced chiral induction when enantiomerically pure pentadienyl ligands

are employed; it is therefore surprising that chiral pentadienyl complexes have been neglected in the literature.¹¹ However, starting from the natural product (1R)-(-)-myrtenal (**1**), we have recently reported a series of open metallocenes and mono(pentadienyl) complexes of early to late transition metals bearing the enantiomerically pure dimethylnopadienyl ligand (**3a**).^{11b} Encouraged by this initial result, we are now extending this synthetic approach to other Wittig salts in order to generate several substituted derivatives. By this methodology a ligand library with different steric and electronic properties should be readily accessible. For our initial study, we decided to focus on H and Ph substitution at the 2-position of the pentadienyl moiety. Phenyl substitution was particularly attractive because of potential conjugation with the pentadienyl fragment, and it might also offer an additional binding site for transition metals. In connection with the former aspect, the studies by Tamm on open-indenyl ligands are especially relevant.¹²

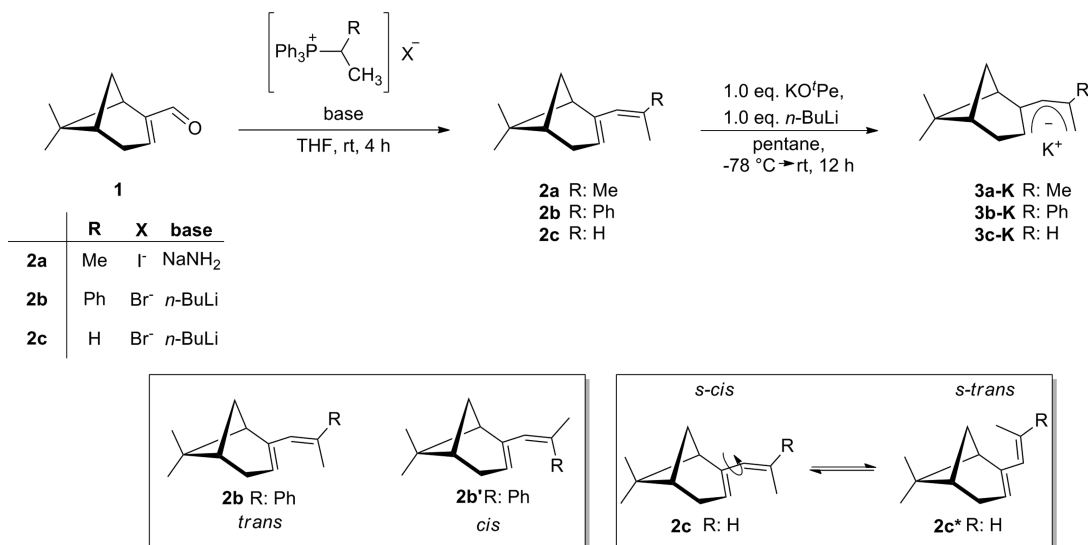
RESULTS AND DISCUSSION

Synthesis and Solution Characterization: Pentadienyls. The natural product (1R)-(-)-myrtenal (**1**) serves as an ideal starting material for the construction of a ligand library. Scheme 1 shows the conversion of **1** with the Wittig salts $[\text{Ph}_3\text{PCH(R)(CH}_3)]\text{I}$ ($\text{R} = \text{Me}$ (**a**), Ph (**b**), H (**c**)) in the presence of an appropriate base such as NaNH_2 or $n\text{-BuLi}$ to give the enantiomerically pure pentadienes **2a**,¹¹ **2b**, and **2c** as colorless oils in good yield. Most notable is the formation of two isomers for **2b/2b'** (in the ratio 4/1) and **2c/2c*** (in the ratio 2.8/1), respectively. The GC/MS retention times of the isomers **2b/2b'** and **2c/2c*** are very different, with $\Delta t = 2.04$ and 0.26

Received: May 14, 2014

Published: July 17, 2014

Scheme 1



min, respectively, suggesting two different kinds of isomers. This hypothesis can further be substantiated by NOESY spectroscopy. Isomers **2b,b'** result from *trans*- and *cis*-Wittig olefinations,¹³ whereas the isomers **2c,c*** correspond to the *s-cis* and *s-trans* conformers¹⁴ of the 1,3-pentadiene (see the Experimental Section for details). Selected ¹H and ¹³C{¹H} NMR resonances of **2a–c** are given in Table 1. As expected, the ¹H and ¹³C{¹H} NMR chemical shifts of the 1,3-diene moieties in **2a–c** vary only within a small chemical shift window, whereas the most pronounced differences between the *cis/trans* and *s-cis/s-trans* isomers of **2b,b'** and **2c,c***, respectively, are observed for the ¹³C{¹H} NMR resonances of C1 and C9 (see Table 1).

Deprotonation of **2a–c** with potassium *tert*-pentoxyde (KO^tPe) and *n*-butyllithium (*n*-BuLi) gives the potassium salts **3a-K**,^{11b} **3b-K**, and **3c-K** in excellent yields (Scheme 1). The potassium pentadienides are isolated as extremely pyrophoric yellow powders that are very soluble in coordinating solvents such as tetrahydrofuran to form dark orange or dark red solutions. However, they are only sparingly soluble in aromatic solvents such as toluene, and they are insoluble in aliphatic solvents such as hexane and pentane.

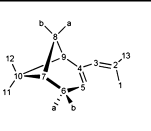
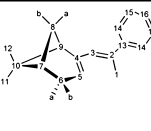
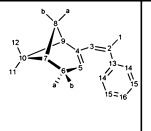
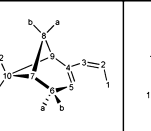
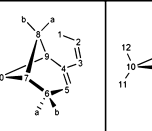
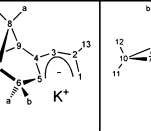
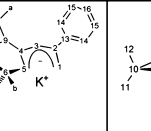

In general, pentadienyl anions can adopt several conformations: namely, the W, S, and U conformations (Chart 1). Several computational and experimental studies have been conducted on alkali-metal pentadienyl and silyl-substituted derivatives in order to elucidate their conformational preference. Density functional theory (DFT) investigations revealed that the η⁵-U conformation is the most stable form for the unsubstituted alkali-metal pentadienyls [(C₅H₇)M] (M = Li–K) in the gas phase. Furthermore, the ground state of these systems is not altered when solvent effects are included in the computations.¹⁵ The preferred conformation of the alkali-metal pentadienyl anions was investigated experimentally in solution by NMR spectroscopy and regioselective trimethylsilylation.^{10a,16} However, only a few alkali-metal pentadienyl complexes have been structurally characterized, such as [(tmeda)K(η⁵-2,4-Me₂C₅H₅)]^{17a} and [(thf)K(μ-η⁵:η⁵-2,4-(Me₃C)₂C₅H₅)]_∞.^{17b} In this complex the U-shaped η⁵-2,4-dimethylpentadienyl anion is coordinated by two potassium cations to form a zigzag polymeric chain in the solid state.¹⁷ Unfortunately, all attempts to crystallize **3a-K–c-K** from saturated THF or tmeda solutions failed, but we succeeded in their solution characterization by 1D- and 2D-NMR

spectroscopy. The ¹H and ¹³C{¹H} NMR resonances of **3a-K–c-K** in THF-*d*₈ are given in Table 1. The hydrogen atoms at the C5 position are observed as a multiplet at δ 3.78–3.73 (**3a-K**), 4.06–3.99 (**3b-K**), and 3.85–3.79 (**3c-K**), whereas those for the central carbon atoms C3 are shifted to high field (**3a-K**, 3.11 ppm; **3b-K**, 3.47 ppm; **3c-K**, 3.19–3.16 ppm). To evaluate the conformation that persists in solution, NOESY NMR experiments were undertaken. The hydrogen atoms attached to C1 can be differentiated into H_{endo} and H_{exo}. The observed NOE interactions are shown in Chart 2, and a representative NOESY NMR spectrum of **3c-K** is shown in Figure 1. The most notable feature is the strong NOE between H5 and H_{endo}, which confirms the U conformation in solution.

However, when crown ether 18-crown-6 was added to toluene suspensions of **3a-K** and **3c-K**, crystals of [K(18-crown-6)][**3a**]^{11b} and [K(18-crown-6)][**3c**] suitable for X-ray diffraction were isolated (see the Supporting Information for details, Table S1) (Scheme 2).

We have previously reported the molecular structure of [K(18-crown-6)][**3a**]^{11b} but for comparison these data will also be included in the discussion. An ORTEP diagram of [K(18-crown-6)][**3c**] is shown in Figure 2, and selected bond distances and angles are given in the figure caption.

Consistent with our solution study, the pentadienyl anions in [K(18-crown-6)][**3a**]^{11b} and [K(18-crown-6)][**3c**] also adopt a U conformation in the solid state. In addition, the C–C distances within the pentadienyl system exhibit a distinct short–long–long–short pattern, and in both cases the pentadienyl anions coordinate to the [K(18-crown-6)]⁺ cation with the less sterically hindered side of the pentadienyl system (viz., *trans* to the CMe₂ bridge). However, K–C bond distances differ substantially, consistent with a change in hapticity. For [K(18-crown-6)][**3a**] the η⁵-U mode was observed with the shortest K–C distance (3.0923(16) Å) to the central C3 atom. The other K–C distances are progressively longer: 3.1156(16) Å (C2), 3.1693(18) Å (C1), 3.2332(16) Å (C4), and 3.3063(18) Å (C5).^{11b} In contrast, [K(18-crown-6)][**3c**] exhibits a η³-U mode with the shortest K–C distance to C2 (3.0015(18) Å) followed by C1 (3.161(2) Å), C3 (3.1284(18) Å), C4 (3.515(2) Å), and C5 (3.799(2) Å). These very long K–C4 and K–C5 distances in [K(18-crown-6)][**3c**] clearly argue for a hapticity switch from

	2a ^{11b}	2b (<i>trans</i>)	2b' (<i>cis</i>)	2c (<i>s-cis</i>)	2c* (<i>s-trans</i>)	3a-K ^{11b}	3b-K	3c-K
								
¹ H NMR Data of 2a , 2b/2b' and 2c/2c* (in CDCl ₃) and 3a-K , 3b-K and 3c-K (in THF- <i>d</i> ₈)								
1	1.78 (br s)	2.12 – 2.09 (m)	2.01 – 1.99 (m)	1.81 – 1.78 (m)	1.79 – 1.74 (m)	3.27–3.22 (m), exo 3.08 (“d”), endo <i>J</i> = 2.76 Hz	3.60 -3.56 (m), exo 3.35 (d), endo <i>J</i> = 2.27 Hz	3.28 (“dd”), exo <i>J</i> = 10.86 Hz <i>J</i> = 1.77 Hz 3.16 – 3.10 (m), endo
2	-	-	-	5.46 – 5.38 (m)	5.61 – 5.51 (m)	-	-	6.00 (ddd) <i>J</i> = 16.60 Hz <i>J</i> = 10.81 Hz <i>J</i> = 8.79 Hz
3	5.57 - 5.53 (m)	6.07 – 6.04 (m)	5.98 – 5.95 (m)	5.78 – 5.72 (m)	6.11 – 6.04 (m)	3.11 (“d”) <i>J</i> = 2.01 Hz	3.47 (“d”) <i>J</i> = 2.02 Hz	3.21 – 3.16 (m)
5	5.38 - 5.34 (m)	5.52 – 5.48 (m)	5.37 – 5.33 (m)	5.51 – 5.47 (m)	5.46 – 5.38 (m)	3.78–3.73 (m)	4.06 – 3.99 (m)	3.86 – 3.79 (m)
6a, 6b	2.37 - 2.26 (m)	2.41 – 2.30 (m)	2.19 – 2.14 (m)	2.45 – 2.34 (m)	2.31 (dt) <i>J</i> = 5.56 Hz <i>J</i> = 1.52 Hz	6a : 2.46 (dt) <i>J</i> = 15.73 Hz <i>J</i> = 2.82 Hz 6b : 2.58 (dt) <i>J</i> = 15.81 Hz <i>J</i> = 3.01 Hz	6a : 2.52 (dt) <i>J</i> = 16.08 Hz <i>J</i> = 2.84 Hz 6b : 2.62 (dt) <i>J</i> = 16.00 Hz <i>J</i> = 2.96 Hz	6a : 2.47 (“dt”) <i>J</i> = 15.92 Hz <i>J</i> = 2.65 Hz 6b : 2.59 (“dt”) <i>J</i> = 15.91 Hz <i>J</i> = 2.90 Hz
7	2.12 - 2.06 (m)	2.07 -2.01 (m)	1.89 – 1.83 (m)	2.16 – 2.07 (m)	2.16 – 2.07 (m)	2.07–1.99 (m)	2.10 – 2.03 (m)	2.07 – 2.00 (m)
8a	1.21 (d) <i>J</i> = 8.53 Hz	1.19 (d) <i>J</i> = 8.59 Hz	0.95 (d) <i>J</i> = 8.59 Hz	1.24 (d) <i>J</i> = 8.08 Hz	1.16 (d) <i>J</i> = 8.59 Hz	1.28 (d) <i>J</i> = 8.28 Hz	1.34 (d) <i>J</i> = 8.08 Hz	1.32 (d) <i>J</i> = 8.34 Hz
8b	2.42 - 2.37 (m)	2.41 – 2.30 (m)	2.07 – 2.01 (m)	2.45 – 2.34 (m)	2.45 – 2.34 (m)	2.26 (dt) <i>J</i> = 8.20 Hz, <i>J</i> = 5.65 Hz	2.30 (dt) <i>J</i> = 8.08 Hz <i>J</i> = 5.56 Hz	2.26 (dt) <i>J</i> = 8.08 Hz <i>J</i> = 5.68 Hz
			(m)	(m)	(m)			
9	2.19 (dt) <i>J</i> = 5.65 Hz <i>J</i> = 1.51 Hz	2.25 (dt) <i>J</i> = 5.69 Hz <i>J</i> = 1.51 Hz	1.59 (dt) <i>J</i> = 5.69 Hz <i>J</i> = 1.65 Hz	2.31 (dt) <i>J</i> = 5.56 Hz <i>J</i> = 1.26 Hz	2.53 (dt) <i>J</i> = 5.56 Hz <i>J</i> = 1.56 Hz	1.78 – 1.74 (m)	1.93 – 1.87 (m)	1.79 – 1.74 (m)
11	0.89 (s)	0.85 (s)	0.75 (s)	0.91 (s)	0.82 (s)	0.91 (s)	0.95 (s)	0.91 (s)
12	1.23 (s)	1.23 (s)	0.91 (s)	1.32 (s)	1.33 (s)	1.21 (s)	1.23 (s)	1.21 (s)
13	1.76 (br s)	-	-	-	-	1.73 (s)	-	-
14	-	7.35 – 7.30 (m)	-	-	-	-	7.50 – 7.44 (m)	-
15	-	7.25 – 7.18 (m)	-	-	-	-	7.11 – 7.03 (m)	-
16	-	7.14 – 7.09 (m)	-	-	-	-	7.02 – 6.96 (m)	-
¹³ C{ ¹ H} NMR Data of 2a , 2b/2b' and 2c/2c* (in CDCl ₃) and 3a-K , 3b-K and 3c-K (in THF- <i>d</i> ₈)								
1	20.1	18.0	26.9	15.3	18.3	75.7	75.1	75.2
2	133.1	134.7	134.9	130.9	121.3	143.0	148.7	135.9
3	126.4	128.9	128.4	123.9	132.8	82.5	86.2	80.4
4	145.7	145.8	146.3	145.3	146.5	149.4	149.5	150.2
5	120.7	122.9	124.4	122.3	121.2	84.1	82.9	86.9
6	32.0	32.2	32.1	32.0	31.9	32.99	33.2	33.0
7	40.8	40.7	40.4	40.8	41.3	42.5	42.5	42.4
8	31.8	31.8	31.8	31.7	31.5	32.97	33.1	32.9

Nevertheless, the ^1H and ^{13}C NMR spectra of $[\text{K}(\text{18-crown-6})][\mathbf{3a}]$ and $[\text{K}(\text{18-crown-6})][\mathbf{3c}]$ recorded in C_6D_6 show

dx.doi.org/10.1021/om500513m | *Organometallics* 2014, 33, 3792–3803

Chart 1

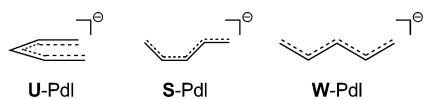
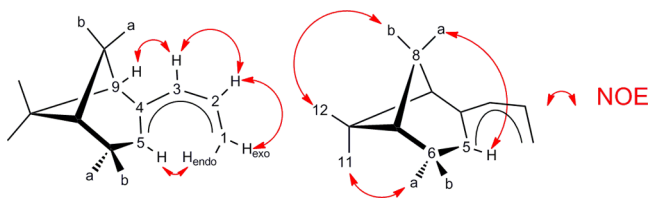


Chart 2



position of the pentadienyl ligand. However, the solution NMR spectra provide no indication of a change in coordination mode ($\eta^5 \rightarrow \eta^3$) as suggested by the solid-state molecular structures of $[\text{K}(18\text{-crown-6})][\mathbf{3a}]$ and $[\text{K}(18\text{-crown-6})][\mathbf{3c}]$, respectively. In addition the NMR spectroscopic data are consistent with either an exclusive coordination of the potassium cation to the less sterically encumbered side of the pentadienyl moiety or alternatively a solvent-separated ion pair.

Reactivity with $[(\eta^7\text{-C}_7\text{H}_7)\text{Zr}(\text{Cl})(\text{tmeda})]$ and Half-Open Troizircene Formation. With these ligands in hand, we set out to prepare transition-metal complexes; our first system of choice was the $(\eta^7\text{-C}_7\text{H}_7)\text{Zr}$ fragment, for several reasons. (1) The half-sandwich complex $[(\eta^7\text{-C}_7\text{H}_7)\text{Zr}(\text{Cl})(\text{tmeda})]$ is an ideal starting point for reactions with monoanionic ligands, including pentadienyls.^{11b,12b,18} (2) The resulting complexes exhibit excellent crystallization properties, which facilitate the structural characterization. (3) The $(\eta^7\text{-C}_7\text{H}_7)\text{Zr}$ fragment can be used to evaluate the steric demand of η^5 -bound monoanionic ligands.^{18f,k}

Previously, we prepared the half-open troizircene $[(\eta^7\text{-C}_7\text{H}_7)\text{Zr}(\eta^5\text{-3a})]$ ($\mathbf{4a}$) in moderate yield,^{11b} and this reactivity can also be extended to our new ligands $\mathbf{3b,c}$ to give $\mathbf{4b,c}$, respectively (Scheme 3). Crystals of $\mathbf{4b,c}$ suitable for X-ray diffraction were grown from concentrated pentane solutions at -30°C (see the Supporting Information for details, Table S1), and the molecular structures are shown in Figure 3, while relevant bond distances and angles are given in Table 2. Compound $\mathbf{4b}$ crystallizes with two independent molecules, which are reasonably similar except for slight differences in the

Scheme 2

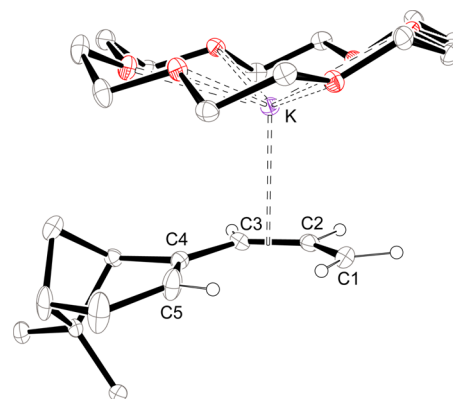
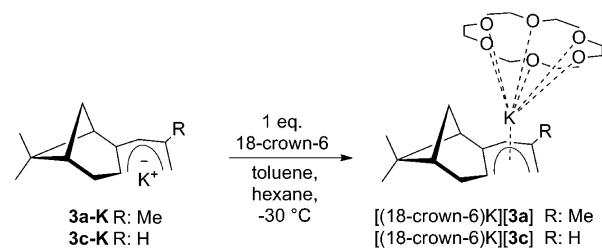


Figure 2. ORTEP diagram of $[\text{K}(18\text{-crown-6})][\mathbf{3c}]$ with thermal displacement parameters drawn at the 30% probability level. Hydrogen atoms, with the exception of those connected to C1–C5, were omitted for clarity. Selected bond lengths (Å) and angles (deg): K–O(18-C-6) 2.8075(13)–3.1284(18), K–C1 3.161(2), K–C2 3.0015(18), K–C3 3.1284(18), K–C4 3.515(2), K–C5 3.799(2), C1–C2 1.367(3), C2–C3 1.407(3), C3–C4 1.424(2), C4–C5 1.358(3); C1–C2–C3 132.8(2), C2–C3–C4 129.34(18), C3–C4–C5 129.28(18).

orientation of the rings. The C–C bond distances (C1–C5) within the pentadienyl ligand exhibit a short–long–long–short pattern similar to that observed in the potassium salts $[\text{K}(18\text{-crown-6})][\mathbf{3a}]$ ^{11b} and $[\text{K}(18\text{-crown-6})][\mathbf{3c}]$ and as previously reported for $[(\eta^7\text{-C}_7\text{H}_7)\text{Zr}(\eta^5\text{-2,4-Me}_2\text{C}_5\text{H}_5)]$.^{18a} Furthermore, the Zr–C distances become progressively longer, starting with Zr–C3 and then moving to Zr–C2/C4 and Zr–C1/C5. This asymmetry in the Zr–C bonds originates from the contraction of the Zr(IV) orbitals, which inhibits an effective interaction with all

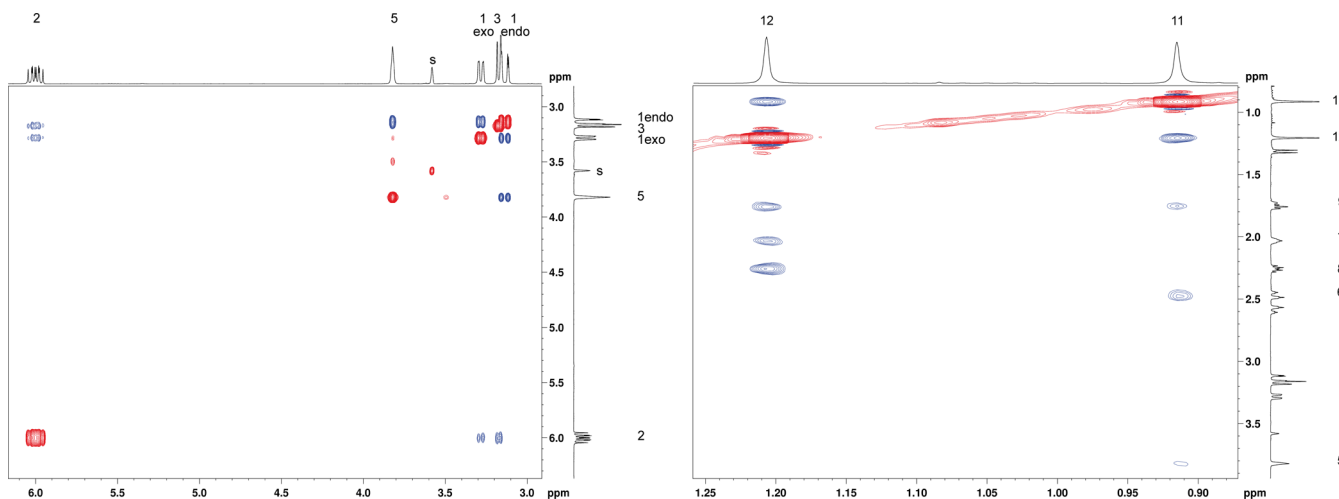


Figure 1. ^1H – ^1H NOESY NMR spectra of $\mathbf{3c-K}$ recorded in $\text{THF-}d_8$.

Scheme 3

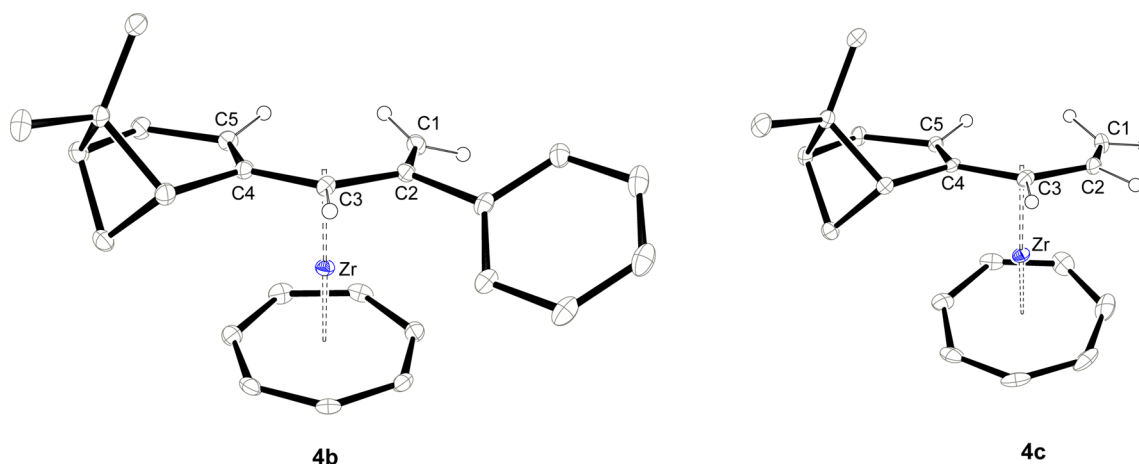
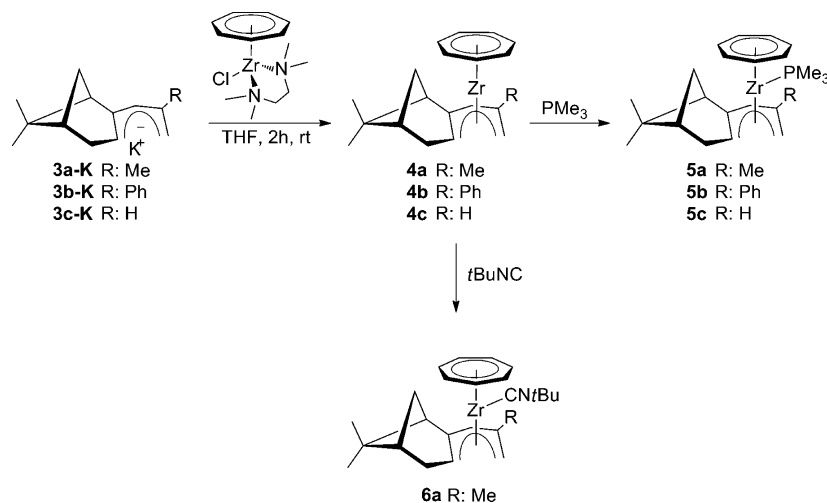


Figure 3. ORTEP diagram of half-open trozircenes **4b,c** with thermal displacement parameters drawn at the 30% probability level. For **4b** only one of the two independent molecules in the asymmetric unit is shown. Hydrogen atoms, with the exception of those connected to C1–C5, are omitted for clarity.

carbon atoms. Furthermore, the less efficient overlap is also reflected in the significantly longer Zr–C4 and Zr–C5 distances in comparison to the corresponding Zr–C2 and Zr–C1 distances and is also a reflection of the asymmetric distribution of the steric bulk in these pentadienyl ligands.

Consistent with our previous study on **4a**,^{11b} the pentadienyl fragments in **4b,c** coordinate exclusively from the sterically less hindered site. Interestingly, a closer inspection of the molecular structure of **4b** reveals close interactions between the two independent molecules in the asymmetric unit. Two H atoms of the C₇H₇ ring of one molecule are directed toward the phenyl ring of the second molecule of **4b**, leading to short C–H... π interactions (2.78–2.90 Å) (see the Supporting Information for a packing diagram). The influence of phenyl-substituted pentadienyl ligands on the crystal packing has previously been discussed in the context of half-open ruthenocene complexes.^{7a}

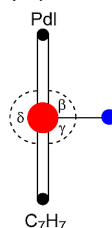
Representative ¹H NMR spectra of **3c-K**, **4c**, and **5c** are shown in Figure 4, and confirm the selective coordination of the pentadienyl ligand **3c** to the (η^7 -C₇H₇)Zr fragment. Upon coordination of pentadienyl **3c** to the (η^7 -C₇H₇)Zr fragment, the ¹H NMR chemical shifts of the Pd moiety (C1–C5) show distinctively different behavior. Whereas the protons H2, H5, and H1_{endo} experience an upfield shift, H3 and H1_{exo} are shifted

downfield. Furthermore, the ¹³C NMR chemical shifts of the carbon atoms C1 and C5 experience only a minor shift on coordination to the (η^7 -C₇H₇)Zr fragment, while the resonances of C2 and C4 are shifted significantly upfield and the C3 carbon atoms are shifted downfield (Table 3). To qualitatively understand these trends, one has to take a closer look at the bonding in these half-open trozircene complexes. The bonding between the Pd fragment and the (η^7 -C₇H₇)Zr fragment occurs between the HOMO and HOMO-1 orbitals of the Pd moiety and the empty d_{xz} and d_{yz} orbitals of the Zr(IV) atom, forming metal– π interactions (Chart 3); for a more detailed discussion the reader may refer to ref 18c. When electron density is transferred from the HOMO of the Pd ligand to the (η^7 -C₇H₇)Zr fragment, a downfield shift in the ¹³C NMR resonances can be expected, whereas the C atoms C2 and C4 are expected to be uninvolved. For the HOMO-1 interaction with the (C₇H₇)Zr fragment the situation is different. The π bonds between C1 and C2 and between C4 and C5, respectively, are expected to be weakened, which lead to an upfield shift of these ¹³C NMR resonances, whereas the resonance at C3 is not affected. These interactions qualitatively rationalize the trends observed in the ¹³C NMR spectra.

Table 2. Selected Bond Distances and Angles for the Half-Open Trozircene Complexes and Their Adducts

	4a ^{11b}	4b ^a	4c	5a	5b	5c ^a	6a
C1–C2	1.3834(15)	1.395(4), 1.389(4)	1.378(3)	1.379(4)	1.387(3)	1.375(6), 1.373(6)	1.381(2)
C2–C3	1.4260(15)	1.428(4), 1.426(4)	1.421(2)	1.431(4)	1.430(3)	1.425(6), 1.424(6)	1.418(2)
C3–C4	1.4368(14)	1.439(3), 1.441(3)	1.432(2)	1.431(3)	1.425(3)	1.423(5), 1.422(5)	1.428(2)
C4–C5	1.3887(14)	1.383(4), 1.377(4)	1.386(2)	1.380(4)	1.382(3)	1.381(6), 1.371(6)	1.382(2)
C1...C5	3.15	3.13, 3.10	3.12	3.14	3.16	3.16, 3.15	3.15
Zr–C1	2.5594(11)	2.557(3), 2.569(3)	2.586(2)	2.598(2)	2.604(2)	2.642(4), 2.632(4)	2.6165(16)
Zr–C2	2.5131(10)	2.510(2), 2.504(2)	2.476(2)	2.558(2)	2.549(2)	2.551(3), 2.545(3)	2.5460(13)
Zr–C3	2.4291(10)	2.455(2), 2.443(2)	2.420(2)	2.509(3)	2.495(3)	2.487(3), 2.486(3)	2.4807(15)
Zr–C4	2.5513(10)	2.563(3), 2.533(2)	2.547(1)	2.599(2)	2.596(2)	2.619(4), 2.618(4)	2.5813(15)
Zr–C5	2.6464(11)	2.670(3), 2.589(3)	2.630(2)	2.663(3)	2.654(2)	2.717(4), 2.702(4)	2.687(1)
Zr–C(av)	2.534 ± 0.070	2.551 ± 0.079, 2.528 ± 0.058	2.532 ± 0.084	2.585 ± 0.057	2.580 ± 0.060	2.603 ± 0.088, 2.597 ± 0.083	2.579 ± 0.072
Zr–P				2.851(7)	2.8556(6)	2.8360(9), 2.8355(9)	
Zr–C21							2.3795(15)
C21–N							1.1526(19)
C22–N							1.4601(19)
PdI(plane)–Zr	2.02	2.02, 1.99	2.01	2.05	2.04	2.09, 2.08	2.06
PdI(cent)–Zr	2.05	2.05, 2.03	2.04	2.10	2.09	2.12, 2.12	2.10
CHT(plane)–Zr	1.69	1.69, 1.69	1.69	1.77	1.78	1.77, 1.78	1.77
CHT(cent)–Zr	1.69	1.69, 1.69	1.69	1.77	1.78	1.80, 1.78	1.77
PdI(plane)–Ph		41, 37					
α(planes)	22	13, 41	24	43	44	42, 42	38
β ^b				99	98	96, 96	94
γ ^b				112	113	116, 116	114
δ ^b				149	148	148, 148	153

^aTwo independent molecules in the asymmetric unit. ^bThe angles β, γ and δ are defined in the following manner:



In principle, CO adducts of groups 4 and 5 open metallocenes can also be used for the evaluation of the electronic properties of these chiral pentadienyls **3a–c**. However, as already demonstrated for $[(\eta^5\text{-3a})_2\text{Ti}]$ and $[(\eta^5\text{-3a})_2\text{V}]$,^{11b} no CO adduct formation was observed, which is probably a consequence of the severe steric demand of these ligands. Nevertheless, Ernst and Tamm extensively explored the electronic structure of half-open trozircenes and their adducts and concluded that there is only minor back-bonding between the formal d^0 Zr(IV) center and additional donor ligands such as isonitriles.^{18a,c} However, this weak interaction leads to small—but measurable—deviations of the $\text{C}\equiv\text{N}$ stretching frequency from the value for the free isonitrile. From these studies it was concluded that the enhanced donor ability of the pentadienyl vs. cyclopentadienyl ligand results in a reduced σ donation from the isonitriles.^{18a,c} Therefore, it should—in principle—be possible to compare different pentadienyl ligands using the $\text{C}\equiv\text{N}$ stretching frequencies. This approach has already been used for pentadienyl (C_5H_7), 2,4-dimethylpentadienyl (C_7H_{11}), and 6,6-dimethylcyclohexadienyl (6,6'-dmch).^{18a,c} A direct comparison between the C–N stretching frequencies of $[(\eta^7\text{-C}_7\text{H}_7)(\eta^5\text{-2,4-Me}_2\text{C}_5\text{H}_5)\text{-Zr}(\text{CNtBu})]$ (2139 cm^{-1})^{18c} and **6a** (2138 cm^{-1}) shows essentially identical values, suggesting that the influence of the chiral moiety on the electronic structure is negligible. Nevertheless, the ^{31}P NMR chemical shift in the PMe_3 adducts **5a–c**

might also serve as a sensitive probe for the electronic structure of these half-open trozircenes. On metal coordination the ^{31}P NMR resonance of PMe_3 is shifted downfield from that of free PMe_3 ($\delta -62.2\text{ ppm}$) and this shift should correlate with the Lewis acidity of the metal center: i.e., the more Lewis acidic the metal, the stronger the shift upon coordination. For **5a–c** a nice progression is observed, in which the most downfield shifted ^{31}P NMR resonance is observed for **5c** ($\delta -45.3\text{ ppm}$) and the least downfield shifted resonance for **5a** ($\delta -49.4\text{ ppm}$) (Table 3). This trend suggests that the Me-substituted ligand **3a** exerts the strongest donating influence on the Zr atom and the H-substituted ligand **3c** the weakest. Nevertheless, substitution at the C2-position has only a minor influence on the electronic structure of these PdI systems, consistent with the fact that these positions are formally “uncharged”.^{7a,19} Crystals of the PMe_3 and $t\text{BuNC}$ adducts are readily obtained from a pentane/thf solvent mixture (2/1) at $-30\text{ }^\circ\text{C}$ (see the Supporting Information for details, Table S1). With the exception of **5c**, all adducts crystallize in the orthorhombic space group $P2_12_12_1$; **5c** crystallizes in the space group $P1$ with two independent molecules, which are closely similar (rms deviation for all non-H atoms 0.02 \AA). The overall structural features of these adducts are rather similar; therefore, only the molecular structures of **5a** and **6a** are shown in Figure 5, whereas the ORTEP diagrams of adducts **5b,c** are

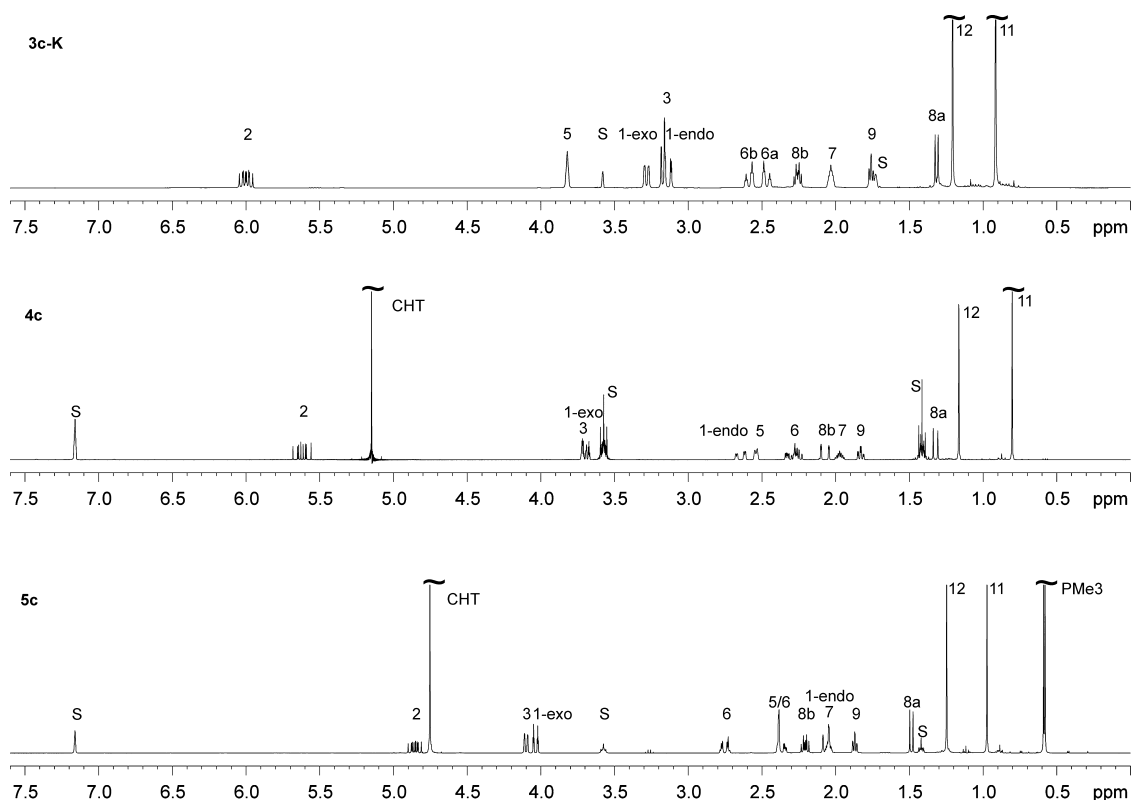


Figure 4. ^1H NMR spectra of **3c-K**, **4c**, and **5c** recorded in $\text{THF-}d_8$ or C_6D_6 . Resonances marked with “S” correspond to residual solvents.

shown in the Supporting Information. Relevant bond distances and angles are given in Table 2.

The Lewis base coordinates from the rear side of the pentadienyl fragment, as observed for $[(\eta^7\text{-C}_7\text{H}_7)(\eta^5\text{-2,4-Me}_2\text{C}_5\text{H}_5)\text{Zr}(\text{NC-}o\text{-Xylyl})]^{18a}$ and $[(\eta^7\text{-C}_7\text{H}_7)(\eta^5\text{-2,4-Me}_2\text{C}_5\text{H}_5)\text{Zr}(\text{L})]$ ($\text{L} = \text{PMe}_3$, $:\text{C}[\text{N}(\text{Me})\text{C}(\text{Me})]_2$).^{18c} Although the overall structure is not changed significantly, the steric constraints force the Zr–C bond distances to increase slightly and the angle α between the C_7H_7 and Pd planes to increase upon coordination by PMe_3 or $t\text{BuNC}$.

Computational Section. Organometallic chemists successfully employ density functional theory (DFT) computations to gain further insights into their experimental studies.²⁰ For our purposes we focused on two aspects: (a) the relative energies of the different Pd conformers and (b) the energy difference in K^+ coordination to the two diastereotopic ligand faces (Chart 4). The latter point relates to the experimentally observed, excellent face selectivity of the myrtenal-derived pentadienyl fragment upon metal coordination. To address these questions, the structures of **3a-K**–**3c-K** were fully optimized at the B97D/6-311G(d,p) level of theory in the gas phase and after inclusion of a solvent continuum model ($\epsilon_r(\text{THF}) = 7.4257$).²¹ The relative Gibbs enthalpies for **3a-K**–**3c-K** are given in Table 4.

The U conformation for the potassium salts **3a-K**–**3c-K** is thermodynamically more favorable than the S and W conformations in the gas phase and after inclusion of a solvent continuum (Table 4). This preference is most pronounced for **3a-K** and least developed for the H-substituted derivative **3c-K**. Furthermore, these DFT calculations also confirm the experimentally observed site preference, in which the K^+ cation preferentially coordinates to the less sterically encumbered pentadienyl face. The question arises if this face preference also persists in other coordination modes and hapticities. Indeed,

after inclusion of solvent effects the DFT calculations predict that K^+ binding from the less sterically encumbered pentadienyl face persists independently of the coordination mode (Table 4). Furthermore, it can also be inferred that **3b-K** and **3c-K** might be able to switch under the proper conditions to the S coordination mode more easily than **3a-K**. In this S coordination K^+ is coordinated in a η^3 fashion to the pentadienyl ligand via C atoms C1–C3 and thereby moves away from the chiral carbon cage, which also reduces steric interactions.

CONCLUSIONS

Enantiomerically pure 1,3-pentadienes are readily prepared by Wittig reactions from (1R)-(–)-myrtenal. Deprotonation of these 1,3-pentadienes with a Schlosser base combination yields the pentadienyl anions **3a–c**, which adopt a U conformation in solution, as shown by NMR spectroscopy, and in the solid state, as illustrated by the molecular structures of the 18-crown-6 adducts $[\text{K}(18\text{-crown-6})][\text{3a}]^{11b}$ and $[\text{K}(18\text{-crown-6})][\text{3c}]$. The coordination chemistry of these new ligands and their electronic properties were evaluated using the $(\eta^7\text{-C}_7\text{H}_7)\text{Zr}$ fragment. These studies confirm the excellent face selectivity of these ligands upon metal coordination, consistent with our previous study on the open metallocenes $[(\eta^5\text{-3a})_2\text{M}]$ ($\text{M} = \text{Ti}, \text{V}, \text{Cr}, \text{Fe}$).^{11b} Furthermore, the electronic and steric properties of the ligands can be modified by changing the substituents at the 2-position of the pentadienyl framework. The changes in steric demand are obvious, while the modifications in the electronic properties required Lewis base adducts to be prepared. From the ^{31}P NMR chemical shifts of **5a–c** it can be concluded that substitution at the 2-position induces only subtle changes, but the donor ability of these pentadienyl ligands **3a–c** decreases in the order **3a** > **3b** > **3c**. DFT computations support the experimental findings and also suggest that a hapticity switch

Table 3. Spectroscopic Details for the Half-Open Trozircenes 3a–c and Their Adducts^a

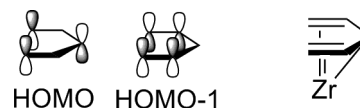
H atom	4a ^{11b}	5a	6a	4b	5b	4c	5c
¹ H NMR Data Recorded in C ₆ D ₆							
1	3.81 (s), exo; 1.87–1.82 (m), endo	4.04–4.00 (m), exo; 1.79–1.80 (m), endo	4.15–4.10 (m), exo; 1.75–1.73 (m), endo	4.35–4.31 (m), exo; 1.88 (d), endo, <i>J</i> = 1.77 Hz	4.56 ("t"), exo, <i>J</i> = 2.46; 1.90 (d), endo, <i>J</i> = 2.46 Hz	3.73–3.66 (m), exo; 2.64 (dd), endo, <i>J</i> = 16.47, 3.03	4.04 (dt), exo, <i>J</i> = 11.29, 1.38; 2.10–2.01 (m), endo
2						5.62 (ddd), <i>J</i> = 16.09, 11.55, 9.28	4.86 (ddd), <i>J</i> = 15.94, 11.41, 8.53
3	3.84 (m)	4.22 ("d"), <i>J</i> = 2.27	4.65 ("d"), <i>J</i> = 2.01	4.42 ("d"), <i>J</i> = 2.78	4.84 ("d"), <i>J</i> = 2.27	3.73–3.66	4.10 ("d"), <i>J</i> = 8.25
5	2.78 (d), <i>J</i> = 4.9	2.58 ("d"), <i>J</i> = 4.73	2.56 ("d"), <i>J</i> = 4.77	2.95 (d), <i>J</i> = 4.29	2.51 ("d"), <i>J</i> = 4.73	2.54 ("d"), <i>J</i> = 4.92	2.42–2.32 (m)
6a, 6b	2.33–2.26 (m), 6a; 2.63 (dd), <i>J</i> = 16.8, 3.4, 6b	2.37 ("ddd"), <i>J</i> = 16.61, 4.69, 2.51, 6a; 2.79 ("ddd"), <i>J</i> = 16.71, 3.08, 1.09, 6b	2.46 ("ddd"), <i>J</i> = 16.56, 4.77, 2.51, 6a; 2.91 ("dd"), <i>J</i> = 16.56, 2.76, 6b	2.38–2.34 (m), 6a; 2.66 (dd), <i>J</i> = 15.92, 3.03, 6b	2.48–2.38 (m), 6a; 2.86 (dd), <i>J</i> = 16.57, 2.75, 6b	2.35–2.22 (m), 6a, 6b	2.42–2.32 (m), 6a; 2.79–2.70 (m), 6b
7	1.99 ("septet")	2.05 ("septet")	2.13–2.05 (m)	2.05–1.99 ("septet")	2.12–2.06 ("septet")	1.97 ("septet")	2.10–2.01 (m)
8a	1.35 (d), <i>J</i> = 9.3	1.44 (d), <i>J</i> = 8.90	1.80 (d), <i>J</i> = 8.90	1.42 (d), <i>J</i> = 9.09	1.51 (d), <i>J</i> = 8.71	1.32 (d), <i>J</i> = 9.28	1.48 (d), <i>J</i> = 8.78
8b	2.33–2.26 (m)	2.17 (dt), <i>J</i> = 8.14, 5.96	2.28 (dt), <i>J</i> = 8.90, 5.96	2.34–2.30 (m)	2.20 (dt), <i>J</i> = 8.80, 5.92	2.11–2.04 (m)	2.21 (dt), <i>J</i> = 8.79, 5.90
9	1.87–1.82 (m)	1.85 (dt), <i>J</i> = 5.68, 1.51	2.13–2.05 (m)	1.95 (dt), <i>J</i> = 5.73, 1.61	2.00 (dt), <i>J</i> = 5.73, 1.42	1.83 (dt), <i>J</i> = 5.68, 1.51	1.87 ("dt")
11	0.81 (s)	0.97 (s)	1.08 (s)	0.83 (s)	1.08 (s)	0.80 (s)	0.97 (s)
12	1.19 (s)	1.24 (s)	1.31 (s)	1.21 (s)	1.30 (s)	1.16 (s)	1.25 (s)
13	1.91 (s)	1.77 ("s")	1.98 (brs)				
14				7.46–7.40 (m)	7.47–7.41 (m)		
15				7.17–7.15 (m)	7.18–7.15 (m)		
16				7.10–6.96 (m)	7.03–6.94 (m)		
CHT	5.16 (s)	4.80 (s)		5.09 (s)	4.71 (s),	5.15 (s)	4.75 (s)
PM _{Me} ₃		0.66 (d), <i>J</i> = 3.22			0.39 (d), <i>J</i> = 3.98,		0.58 (d), <i>J</i> = 3.84
<i>t</i> Bu		0.74					
¹³ C{ ¹ H} NMR Data Recorded in C ₆ D ₆							
1	78.0	78.6	76.5	74.3	77.0	76.8	75.8
2	129.9	121.7	120.3	132.7	134.4	113.8	105.5
3	93.6	90.7	92.3	93.5	89.1	91.9	87.3
4	144.4	136.0	133.8	143.7	145.3	145.1	137.2
5	86.0	86.6	85.5	86.8	87.0	86.5	87.8
6	32.4	31.8	31.9	32.5	31.7	32.5	31.8
7	41.1	41.7	42.0	41.1	41.9	41.1	41.7
8	35.3	34.6	34.4	35.4	34.5	35.2	34.4
9	51.7	51.1	52.1	52.1	51.4	51.1	50.9
10	39.2	39.6	39.7	39.3	39.9	39.3	39.8
11	21.3	21.5	21.6	21.3	21.6	21.3	21.4
12	26.2	26.5	26.6	26.1	26.5	26.1	26.5
13	27.7	27.4	28.2	144.5	124.0		
14				128.0	127.3		
15				128.30	128.2		
16				128.25	126.9		
CHT	82.8	81.4	82.4	83.5	81.9	82.3	80.9
PM _{Me} ₃		18.6 (d), <i>J</i> = 6.3			18.0 (d), <i>J</i> = 8.3		18.4 (d), <i>J</i> = 8.3

Table 3. continued

H atom	4a ^{11b}	5a	6a	4b	5b	4c	5c
CN			¹³ C{ ¹ H} NMR Data Recorded in C ₆ D ₆				
<i>t</i> Bu			151.8				
<i>Ci</i> Bu			29.5				
			54.7				
				³¹ P{ ¹ H} NMR Data Recorded in C ₆ D ₆			
					−47.4		−45.3

^aResonances are given in ppm and *J* values in Hz.

Chart 3



from η^5 to η^3 coordination is feasible in principle for these pentadienyl ligands, but this is also associated with a shift of the K^+ cation to carbon atoms C1–C3 and therefore away from the bicyclic fragment.

We are currently investigating the possibility of this hapticity switch for the pentadienyl systems **3a–c**, along with their additional N-donor functionalization. These results and the coordination chemistry with other d- and f-block elements will be reported in due course.

EXPERIMENTAL SECTION

General Considerations. All experiments were carried out under an atmosphere of purified N_2 , either in a Schlenk apparatus or in a glovebox. The solvents were dried and deoxygenated by distillation under a nitrogen atmosphere from sodium benzophenone ketyl (tetrahydrofuran) and by an MBraun GmbH solvent purification system (toluene, pentane). The following starting materials were prepared according to literature procedures: KO^iPr ,²² $[(\eta^7-C_7H_7)Zr(tmeda)Cl]$,^{18a} $[K(18-crown-6)][3a]$,^{11b} and $[(\eta^7-C_7H_7)Zr(\eta^5-3a)]$ (**4a**).^{11b} Other commercial reagents as *n*-BuLi (Acros), 18-crown-6 ether (Acros), $[Ph_3PCH(CH_3)_2]I$ (Sigma-Aldrich), (1*R*)-(−)-myrtenal (**1**) (Sigma-Aldrich), and $NaNH_2$ (Acros) were used as received without further purification.

NMR spectra were recorded on a Bruker DRX 400 spectrometer at 400 MHz (¹H) or 101 MHz (¹³C). All chemical shifts are reported in δ units with reference to the residual protons of the deuterated solvents, which are internal standards, for proton and carbon chemical shifts. Gas chromatography was performed with a Hewlett-Packard 5890 Series II instrument, using a 35 m \times 0.25 mm glass capillary column coated with Cyclodex-B. Elemental analyses were performed on a Vario MICRO cube elemental analyzer (MS Finnigan MAT 8400-MSS I and Finnigan MAT 4515).

X-ray Diffraction Studies. Data were recorded at 100(2) K on Oxford Diffraction diffractometers using monochromated Mo $K\alpha$ or mirror-focused Cu $K\alpha$ radiation (see the Supporting Information for details, Table S1). The structures were refined anisotropically using the SHELXL-97 program.²³ Hydrogen atoms of the seven-membered rings and at the coordinating C atoms of the novel ligands were refined freely; other H atoms were included using rigid methyl groups or a riding model. The absolute configuration was confirmed for each structure by the Flack parameter. Special features and exceptions are as follows. For **4c**, the seven-membered ring is disordered over two positions. Hydrogen atoms of the ring were included using a riding model. An appropriate system of restraints was employed to stabilize the refinement, but the dimensions of disordered groups should be interpreted with caution. The crystal of **5c** was nonmerohedrally twinned by a 180° rotation about $[110]$. Refinement was implemented using the “HKLF 5” method. The relative volume of the minor twinning component refined to 0.203(1). Reflection numbers are not well-defined for nonmerohedral twins because of differing degrees of reflection overlap.

Synthesis of $[Ph_3PCH_2CH_3]Br$. A solution of PPh_3 (26.2 g, 100 mmol) in 250 mL of EtBr (3350 mmol) was stirred under reflux for 5 days. During this time a colorless precipitate formed, which was filtered off and dried under dynamic vacuum. Yield: 32.3 g (87 mmol, 87%). Anal. Calcd for $C_{20}H_{20}PBr$ (371.24): C, 64.70; H, 5.43. Found: C, 64.50; H, 5.48. ³¹P{¹H} NMR (121 MHz, C₆D₆, ambient): δ 26.7 ppm.

Synthesis of $[Ph_3PCH(CH_3)Ph]Br$. To a solution of PPh_3 (14.2 g, 54 mmol) in toluene (250 mL) was added (1-bromoethyl)benzene (10 g, 54 mmol). This solution was stirred under reflux for 5 days. During this time a colorless solid was formed, which was filtered off, washed with toluene (200 mL), and dried under dynamic vacuum. Yield: 18.1 g (40.5

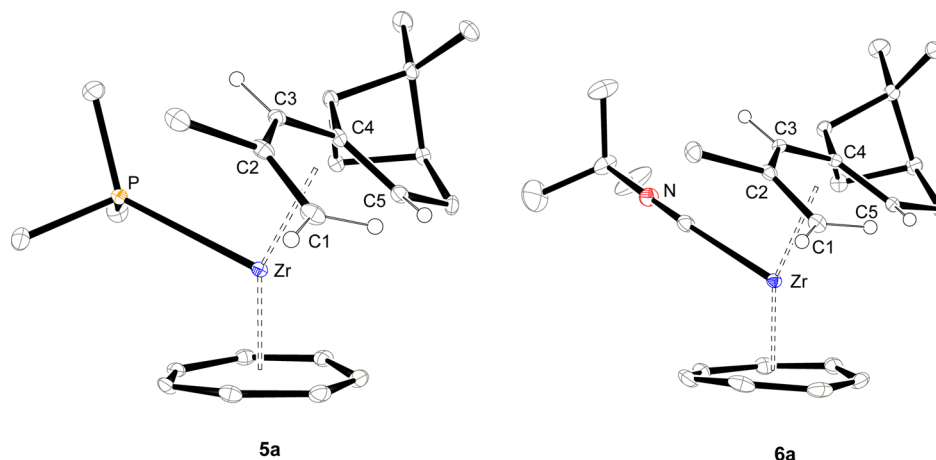


Figure 5. ORTEP diagrams of half-open trozircenes **5a** and **6a** with thermal displacement parameters drawn at the 30% probability level. Hydrogen atoms, with the exception of those connected to C1–C5, are omitted for clarity.

Chart 4

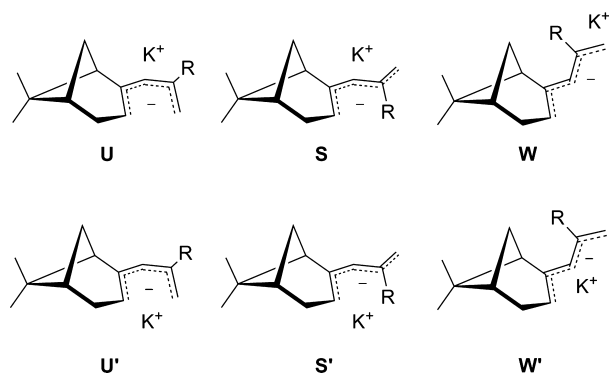


Table 4. Relative Free Gibbs Enthalpies (ΔG°) of the Different Conformers and Diastereomers of **3a-K–c-K⁺**

	3a-K	3b-K	3c-K
U	0.00 [0.00]	0.00 [0.00]	0.00 [0.00]
U'	0.52 [0.83]	0.39 [0.78]	0.39 [1.04]
S	5.12 [5.01]	2.37 [2.67]	3.72 [2.89]
S'	5.17 [5.42]	2.46 [6.49]	5.59 [7.48]
W	8.81 [7.99]	6.33 [4.73]	5.64 [3.66]
W'	8.77 [8.20]	6.33 [5.95]	5.62 [3.67]

^aEnergy values given in brackets correspond to values obtained after inclusion of a solvent continuum (THF). The prime (') denotes K⁺ coordination *syn* to the CMe₂ bridge.

mmol, 75%). Anal. Calcd for C₂₆H₂₄PBr (447.33): C, 69.81; H, 5.41. Found: C, 69.65; H, 5.36. ³¹P{¹H} NMR (121 MHz, C₆D₆, ambient): δ 27.7 ppm.

Standard Procedure for the Synthesis of Enantiomerically Pure 1,3-Pentadienes (2a–c). A suspension of the phosphonium salt [Ph₃PCH(CH₃)(R)]I (R = Me (a); 50 mmol) and NaNH₂ (50 mmol) in THF (250 mL) was stirred at ambient temperature. For the phosphonium salts [Ph₃PCH(CH₃)(R)]Br (R = Ph (b), H (c); 50 mmol) deprotonation was accomplished by the addition of *n*-BuLi (50 mmol) to a THF suspension (250 mL) at –78 °C. The suspension turned brown after a few minutes, and stirring was continued for 12 h until a clear solution was formed. (1R)-(–)-myrtenal (**1**; 50 mmol) was added, and the solution was stirred at ambient temperature for 4 h. The yellow to orange solutions were poured into a diethyl ether/water mixture (100 mL/100 mL). The ether phase was separated, and the water phase was extracted with three portions of diethyl ether (30 mL). The collected organic phases were washed with a 40% aqueous NaHSO₃

solution (20 mL) and dried over NaHCO₃, yielding a pale yellow solution. After removal of the solvent, pentane (250 mL) was added to precipitate Ph₃PO. Filtration, removal of the solvent, and column chromatography (silica, pentane) yielded the enantiomerically pure 1,3-pentadienes **2a–c** as colorless oils. Mixtures of *cis* and *trans* or *s-cis* and *s-trans* isomers were obtained for the 1,3-dienes **2b/2b'** and **2c/2c'**, respectively.

2a: yield 82%; *R_f*(pentane) = 0.86; GC/MS 22.64 min; HRMS calcd 176.15650, found 176.15631. Anal. Calcd for C₁₃H₂₀ (176.30): C, 88.56; H, 11.43. Found: C, 86.01; H, 10.88.

2b/2b': total yield 84%; mixture of *trans* (**2b**) and *cis* (**2b'**) isomers in a 4.26:1 ratio; *R_f*(pentane) = 0.55 (**2b**) and 0.32 (**2b'**); GC/MS 20.03 min (**2b**) and 17.99 (**2b'**); HRMS: calcd 238.16982, found 238.17215. Anal. Calcd for C₁₈H₂₂ (238.37): C, 90.70; H, 9.30. Found: C, 90.69; H, 9.35.

2c/2c': total yield 76%; mixture of *s-cis* (**2c**) and *s-trans* (**2c'**) isomers in a 2.85:1 ratio; *R_f*(pentane) = 1.00 (**2c**) and 0.91 (**2c'**); GC/MS 10.72 min (**2c**) and 10.98 (**2c'**); HRMS: calcd 162.14085, found 162.13863. Anal. Calcd for C₁₂H₁₈ (162.27): C, 88.82; H, 11.18. Found: C, 86.42; H, 10.93.

Standard Procedure for the Synthesis of Potassium Pentadienides (3a-K–c-K). A solution of KO⁺Pen (1 equiv, 35 mmol) in pentane (200 mL) was prepared, and *n*-BuLi (1 equiv, 35 mmol) was added at –78 °C. After the mixture was stirred for 10 min at –78 °C, the 1,3-diene (1 equiv, 35 mmol) was added. The reaction mixture was warmed slowly to room temperature and was stirred at this temperature for 12 h. During this time a color change to yellow was observed. For the phenyl-substituted 1,3-pentadienide **3b-K** the reaction mixture turned red and a yellow precipitate was formed. After filtration, the yellow precipitates were washed with pentane (3 × 20 mL) and dried under dynamic vacuum to yield **3a-K–c-K** as highly pyrophoric yellow solids.

3a-K: yield 90%. Anal. Calcd for C₁₃H₁₉K (214.39): C, 72.83; H, 8.93. Found: C, 70.67; H, 8.85.

3b-K: yield 86%. Anal. Calcd for C₁₈H₂₁K (276.46): C, 78.20; H, 7.66. Found: C, 75.85; H, 7.16.

3c-K: yield 74%. Anal. Calcd for C₁₂H₁₇K (200.37): C, 71.97; H, 8.56. Found: C, 70.53; H, 8.34.

Despite several attempts, no better analytical results could be obtained, which is probably attributable to the extreme air and moisture sensitivity of these potassium salts.

Synthesis of (18-Crown-6)potassium Methyl(phenyl)-nopadienide ([K(18-crown-6)][3c]). The synthesis of ([K(18-crown-6)][3c]) was carried out in a manner identical with that of ([K(18-crown-6)][3a]). 18-Crown-6 ether (197.9 mg, 0.749 mmol) in toluene (1.0 mL) and **3c-K** (150 mg, 0.749 mmol) were reacted. Crystals were grown from a toluene/pentane mixture (1/1) at –23 °C. Yield: 213.3 mg (0.459 mmol, 61%). Anal. Calcd for C₂₄H₄₁KO₆: C, 62.03; H, 8.89. Found: C, 61.34; H, 8.88. ¹H NMR (400 MHz, C₆D₆,

298 K): δ 6.74 (ddd, 1 H, J = 16.31, 10.54, 8.78 Hz, H2), 4.50 ("brs", 1 H, H3), 4.13 (dd, 1 H, J = 16.19 (trans), 2.89 Hz, H1-endo), 3.95 (dd, 1 H, J = 10.66 (cis), 2.64 Hz, H1-exo), 3.87 (d, 1 H, J = 8.78 Hz, H5), 3.23 (s, 24 H, 18-crown-6), 3.11–3.00 (m, 2 H, H6), 2.57–2.49 (m, 2 H, H7 and H8b), 2.41–2.35 (m, 1 H, H9), 1.85 ("d", 1 H, J = 6.53 Hz, H8a), 1.63 (s, 3 H, H12), 1.58 (s, 3 H, H11) ppm. $^{13}\text{C}\{^1\text{H}\}$ NMR (101 MHz, C_6D_6 , ambient): δ 150.9 (C, C4), 136.9 (CH, C2), 84.8 (CH, C3), 81.3 (CH, C5), 76.7 (CH_2 , C1), 70.2 (CH_2 , 18-crown-6-ether), 53.5 (CH, C9), 42.9 (CH, C7), 39.9 (C, C10), 33.9 (CH_2 , C6), 31.7 (CH_2 , C8), 27.9 (CH_3 , C12), 22.1 (CH_3 , C11) ppm.

Synthesis of $[(\eta^7\text{-C}_7\text{H}_7)\text{Zr}(\eta^5\text{-3b})]$ (4b). The synthesis of 4b was carried out in a manner identical with that for 4a, using $[(\eta^7\text{-C}_7\text{H}_7)\text{ZrCl}(\text{tmeda})]$ (100 mg, 0.299 mmol) in THF (10 mL) and 3c (83.6 mg, 0.299 mmol). Yield: 22 mg (0.052 mmol, 18%). Mp: 158 °C dec. Anal. Calcd for $\text{C}_{23}\text{H}_{28}\text{Zr}$: C, 71.54; H, 6.72. Found: C, 70.28; H, 7.05.

Synthesis of $[(\eta^7\text{-C}_7\text{H}_7)\text{Zr}(\eta^5\text{-3c})]$ (4c). $[(\eta^7\text{-C}_7\text{H}_7)\text{ZrCl}(\text{tmeda})]$ (50 mg, 0.15 mmol) was dissolved in THF (5 mL). Addition of 3c (30 mg, 0.14 mmol), dissolved in THF (5 mL), resulted in a dark red to brown suspension. After the mixture was stirred at ambient temperature for 2 h, the solvent was removed. The brown residue was extracted with 2 mL of pentane. Concentration of the extract to 1 mL and cooling to -30 °C resulted in bright red crystals. Yield: 47.1 mg (0.137 mmol, 92%). Mp: 135–138 °C dec. Anal. Calcd for $\text{C}_{19}\text{H}_{24}\text{Zr}$: C, 66.4; H, 7.04. Found: C, 66.0; H, 7.06.

Synthesis of $[(\eta^7\text{-C}_7\text{H}_7)\text{Zr}(\eta^5\text{-3a})(\text{PMe}_3)]$ (5a). $[(\eta^7\text{-C}_7\text{H}_7)\text{Zr}(\eta^5\text{-3a})]$ (32 mg, 0.089 mmol) was dissolved in pentane (1 mL) and THF (0.5 mL). After addition of 6.7 mg (0.089 mmol) of PMe_3 the solution changed from dark brown to orange. Cooling to -30 °C of the solution resulted in bright orange crystals. Yield: 32.9 mg (0.076 mmol, 85%). Mp: 154 °C dec. Anal. Calcd for $\text{C}_{23}\text{H}_{33}\text{PZr}$: C, 63.69; H, 8.13. Found: C, 63.13; H, 7.51.

Synthesis of $[(\eta^7\text{-C}_7\text{H}_7)\text{Zr}(\eta^5\text{-3b})(\text{PMe}_3)]$ (5b). $[(\eta^7\text{-C}_7\text{H}_7)\text{Zr}(\eta^5\text{-3b})]$ (56 mg, 0.134 mmol) was dissolved in pentane (1 mL) and THF (0.5 mL). On addition of PMe_3 (10.2 mg, 0.134 mmol) a bright orange suspension was formed. The precipitate was dissolved with a few drops of THF. Concentration of the extract to ca. 0.5 mL and cooling to -30 °C resulted in bright orange crystals. Yield: 41.6 mg (0.084 mol, 63%). Mp: 161 °C dec. Anal. Calcd for $\text{C}_{28}\text{H}_{37}\text{PZr}$: C, 67.83; H, 7.52. Found: C, 67.49; H, 7.43.

Synthesis of $[(\eta^7\text{-C}_7\text{H}_7)\text{Zr}(\eta^5\text{-3c})(\text{PMe}_3)]$ (5c). $[(\eta^7\text{-C}_7\text{H}_7)\text{Zr}(\eta^5\text{-3c})]$ (46 mg, 0.134 mmol) was dissolved in 1 mL of pentane and 0.5 mL of THF. After addition of 10.2 mg (0.134 mmol) of PMe_3 the solution changed from dark brown to orange. Cooling to -30 °C resulted in intensely orange crystals. Yield: 92% (51.8 mg, 0.123 mmol). Mp: 150 °C dec. Anal. Calcd for $\text{C}_{22}\text{H}_{33}\text{PZr}$: C, 62.96; H, 7.93. Found: C, 62.55; H, 7.80.

Synthesis of $[(\eta^7\text{-C}_7\text{H}_7)\text{Zr}(\eta^5\text{-3a})(\text{CNtBu})]$ (6a). $[(\eta^7\text{-C}_7\text{H}_7)\text{Zr}(\eta^5\text{-3a})]$ (31.4 mg, 0.088 mmol) was dissolved in pentane (1 mL) and THF (0.5 mL). After addition of 7.3 mg (0.088 mmol) of tBuNC the solution changed from dark brown to orange. Cooling of this solution to -30 °C resulted in bright orange crystals. Yield: 35 mg (0.079 mmol, 90%). Anal. Calcd for $\text{C}_{25}\text{H}_{36}\text{NZr}$: C, 67.97; H, 8.21; N, 3.17. Found: C, 66.11; H, 8.06; N, 3.50. IR (KBr): 2138 cm^{-1} (NC).

Computational Details. All calculations were carried out with Gaussian 09²⁴ and the long-range dispersion-corrected Grimme functional B97D.^{24,25} No symmetry restrictions were imposed (C_1). C, H, and N were represented by an all-electron 6-311G(d,p) basis set. The structures were fully optimized in the gas phase and after inclusion of a solvent continuum model ($\epsilon_r(\text{THF}) = 7.4257$).²¹ The nature of the extrema (minima) was established with analytical frequency calculations. The zero point vibration energy (ZPE) and entropic contributions were estimated within the harmonic potential approximation. The Gibbs free energy, ΔG , was calculated for $T = 298.15$ K and 1 atm. Geometrical parameters were reported within an accuracy of 10^{-3} Å and 10^{-1} deg.

■ ASSOCIATED CONTENT

Supporting Information

Tables, figures, and CIF and .mol files giving crystallographic data for $[\text{K}(18\text{-crown-6})][3\text{c}]$, 4b,c, 5a–c and 6a, a packing diagram of 4b, ORTEP diagrams of 5b,c, and computational details. This material is available free of charge via the Internet at <http://pubs.acs.org>.

■ AUTHOR INFORMATION

Corresponding Author

*E-mail for M.D.W.: mwalter@tu-bs.de.

Present Address

[†]Faculty of Chemistry, Alexandru Ioan Cuza University of Iași, 11, Carol 1, 700506 Iași, Romania.

Author Contributions

The manuscript was written through contributions of all authors. All authors have given approval to the final version of the manuscript.

Notes

The authors declare no competing financial interest.

■ ACKNOWLEDGMENTS

This work was supported by the TU Braunschweig through the "Zukunftsfonds" and by the Deutsche Forschungsgemeinschaft (DFG) through the Emmy-Noether program (WA 2513/2).

■ REFERENCES

- (a) Hartwig, J. F. *Organotransition Metal Chemistry: From Bonding to Catalysis*; University Science: Sausalito, CA, 2010; (b) Togni, A.; Haltermann, W. A. *Metalloenes*; Wiley-VCH: Weinheim, Germany, 1998. (c) Brintzinger, H. H.; Fischer, D.; Mülhaupt, R.; Rieger, B.; Waymouth, R. M. *Angew. Chem., Int. Ed. Engl.* **1995**, *34*, 1143. (d) Giardello, M. A.; Eisen, M. S.; Stern, C. L.; Marks, T. J. *J. Am. Chem. Soc.* **1995**, *117*, 12114. (e) Bochmann, M. *J. Chem. Soc., Dalton Trans.* **1996**, 255. (f) Kaminsky, W.; Arndt, M. In *Polymer Synthesis/Polymer Catalysis*; Springer: Berlin, Heidelberg, 1997; Vol. 127, p 143. (g) Janiak, C.; Schumann, H. *Adv. Organomet. Chem.* **1991**, *33*, 290.
- (2) Siemeling, U. *Chem. Rev.* **2000**, *100*, 1495.
- (3) Cesarotti, E.; Kagan, H. B.; Goddard, R.; Krüger, C. *J. Organomet. Chem.* **1978**, *162*, 297.
- (4) Wilson, D. R.; DiLullo, A. A.; Ernst, R. D. *J. Am. Chem. Soc.* **1980**, *102*, 5928.
- (5) (a) Ernst, R. D. *Struct. Bonding (Berlin)* **1984**, *57*, 1. (b) Ernst, R. D. *Acc. Chem. Res.* **1985**, *18*, 56. (c) Ernst, R. D. *Chem. Rev.* **1988**, *88*, 1255. (d) Ernst, R. D. *Comments Inorg. Chem.* **1999**, *21*, 285. (e) Stahl, L.; Ernst, R. D. *Adv. Organomet. Chem.* **2007**, *55*, 137.
- (6) (a) Ceccon, A.; Gambaro, A.; Venzo, A. *J. Chem. Soc., Chem. Commun.* **1985**, 540. (b) Powell, P. J. *Organomet. Chem.* **1981**, *206*, 239. (c) Powell, P. J. *Organomet. Chem.* **1983**, *244*, 393. (d) Powell, P.; Stephens, M.; Muller, A.; Drew, M. G. B. *J. Organomet. Chem.* **1986**, *310*, 255. (e) Donaldson, W. A.; Ramaswamy, M. *Tetrahedron Lett.* **1989**, *30*, 1339.
- (7) (a) Kulsomphob, V.; Turpin, G. C.; Lam, K.-C.; Youngkin, C.; Trakarnpruk, W.; Carroll, P.; Rheingold, A. L.; Ernst, R. D. *J. Chem. Soc., Dalton Trans.* **2000**, 3086. (b) Turpin, G. C.; Rheingold, A. L.; Ernst, R. D. *J. Organomet. Chem.* **2003**, *672*, 109.
- (8) Kulsomphob, V.; Tomaszewski, R.; Yap, G. P. A.; Liable-Sands, L. M.; Rheingold, A. L.; Ernst, R. D. *J. Chem. Soc., Dalton Trans.* **1999**, 3995.
- (9) (a) Bleeke, J. R. *Organometallics* **2005**, *24*, 5190. (b) Rajapakshe, A.; Paz-Sandoval, M. A.; Gutierrez, J. A.; Navarro-Clemente, M. E.; Saavedra, P. J.; Gruhn, N. E.; Lichtenberger, D. L. *Organometallics* **2006**, *25*, 1914. (c) Bleeke, J. R. *Acc. Chem. Res.* **2007**, *40*, 1035. (d) Reyna-Madrigal, A.; Moreno-Gurrola, A.; Perez-Camacho, O.; Navarro-Clemente, M. E.; Juarez-Saavedra, P.; Leyva-Ramirez, M. A.; Arif, A. M.; Ernst, R. D.; Paz-Sandoval, M. A. *Organometallics* **2012**, *31*, 7125.

- (e) Cruz-Cruz, J. I. d. I.; Romano-Tequimila, J. C.; Juarez-Saavedra, P.; Paz-Sandoval, M. A. Z. *Anorg. Allg. Chem.* **2013**, 639, 1160.
- (10) (a) Yasuda, H.; Nakamura, A. *J. Organomet. Chem.* **1985**, 285, 15. (b) Powell, P. *Adv. Organomet. Chem.* **1986**, 26, 125.
- (11) (a) Bosch, H. W.; Hund, H.-U.; Nietlispach, D.; Salzer, A. *Organometallics* **1992**, 11, 2087. (b) Fecker, A. C.; Glöckner, A.; Daniliuc, C. G.; Freytag, M.; Jones, P. G.; Walter, M. D. *Organometallics* **2013**, 32, 874.
- (12) (a) Glöckner, A.; Arias, O.; Bannenberg, T.; Daniliuc, C. G.; Jones, P. G.; Tamm, M. *Dalton Trans.* **2011**, 40, 11511. (b) Glöckner, A.; Bannenberg, T.; Ibrom, K.; Daniliuc, C. G.; Freytag, M.; Jones, P. G.; Walter, M. D.; Tamm, M. *Organometallics* **2012**, 31, 4480.
- (13) Brückner, R. *Reaktionsmechanismen: Organische Reaktionen, Stereochemie, moderne Synthesemethoden*; Spektrum, Acad. Verl.: Heidelberg, 1996.
- (14) Moss, G. P. *Pure Appl. Chem.* **1996**, 68, 2193.
- (15) Cerpa, E.; Tenorio, F. J.; Contreras, M.; Villanueva, M.; Beltran, H. I.; Heine, T.; Donald, K. J.; Merino, G. *Organometallics* **2008**, 27, 827.
- (16) (a) Heiszwolf, G. J.; Kloosterziel, H. *Recl. Trav. Chim. Pays-Bas* **1967**, 86, 807. (b) Kloosterziel, H.; Van, D. M. J. A. A. *Recl. Trav. Chim. Pays-Bas* **1970**, 89, 270. (c) Yasuda, H.; Ohnuma, Y.; Yamauchi, M.; Tani, H.; Nakamura, A. *Bull. Chem. Soc. Jpn.* **1979**, 52, 2036. (d) Yasuda, H.; Yamauchi, M.; Nakamura, A.; Sei, T.; Kai, Y.; Yasuoka, N.; Kasai, N. *Bull. Chem. Soc. Jpn.* **1980**, 53, 1089. (e) Yasuda, H.; Yamauchi, M.; Ohnuma, Y.; Nakamura, A. *Bull. Chem. Soc. Jpn.* **1981**, 54, 1481. (f) Yasuda, H.; Nishi, T.; Lee, K.; Nakamura, A. *Organometallics* **1983**, 2, 21. (g) Schlosser, M.; Staehle, M. *Angew. Chem.* **1982**, 94, 142. (h) Schlosser, M.; Lehmann, R.; Jenny, T. J. *Organomet. Chem.* **1990**, 389, 149. (i) Solomon, S. A.; Bickelhaupt, F. M.; Layfield, R. A.; Nilsson, M.; Poater, J.; Solà, M. *Chem. Commun.* **2011**, 47, 6162. (j) Day, B. M.; Clayden, J.; Layfield, R. A. *Organometallics* **2013**, 32, 4448.
- (17) (a) Gong, L.; Hu, N.; Jin, Z.; Chen, W. J. *Organomet. Chem.* **1988**, 352, 62. (b) Reiners, M.; Fecker, A. C.; Freytag, M.; Jones, P. G.; Walter, M. D. *Dalton Trans.* **2014**, 43, 6614.
- (18) (a) Glöckner, A.; Bannenberg, T.; Tamm, M.; Arif, A. M.; Ernst, R. D. *Organometallics* **2009**, 28, 5866. (b) Glöckner, A.; Tamm, M.; Arif, A. M.; Ernst, R. D. *Organometallics* **2009**, 28, 7041. (c) Glöckner, A.; Arif, A. M.; Ernst, R. D.; Bannenberg, T.; Daniliuc, C. G.; Jones, P. G.; Tamm, M. *Inorg. Chim. Acta* **2010**, 364, 23. (d) Glöckner, A.; Bannenberg, T.; Büschel, S.; Daniliuc, C. G.; Jones, P. G.; Tamm, M. *Chem. Eur. J.* **2011**, 17, 6118. (e) Glöckner, A.; Bannenberg, T.; Daniliuc, C. G.; Jones, P. G.; Tamm, M. *Inorg. Chem.* **2012**, 51, 4368. (f) Glöckner, A.; Bauer, H.; Maekawa, M.; Bannenberg, T.; Daniliuc, C. G.; Jones, P. G.; Sun, Y.; Sitzmann, H.; Tamm, M.; Walter, M. D. *Dalton Trans.* **2012**, 41, 6614. (g) Glöckner, A.; Cui, P.; Chen, Y.; Daniliuc, C. G.; Jones, P. G.; Tamm, M. *New J. Chem.* **2012**, 36, 1392. (h) Glöckner, A.; Daniliuc, C. G.; Freytag, M.; Jones, P. G.; Tamm, M. *Chem. Commun.* **2012**, 48, 6598. (i) Glöckner, A.; Kronig, S.; Bannenberg, T.; Daniliuc, C. G.; Jones, P. G.; Tamm, M. *J. Organomet. Chem.* **2012**, 723, 181. (j) Glöckner, A.; Tamm, M. *Chem. Soc. Rev.* **2012**, 42, 128. (k) Kreye, M.; Glöckner, A.; Daniliuc, C. G.; Freytag, M.; Jones, P. G.; Tamm, M.; Walter, M. D. *Dalton Trans.* **2013**, 42, 2192.
- (19) (a) Newbound, T. D.; Rheingold, A. L.; Ernst, R. D. *Organometallics* **1992**, 11, 1693. (b) Gedridge, R. W.; Hutchinson, J. P.; Rheingold, A. L.; Ernst, R. D. *Organometallics* **1993**, 12, 1553.
- (20) (a) Davidson, E. R. *Chem. Rev.* **2000**, 100, 351. (b) Lin, Z. *Acc. Chem. Res.* **2010**, 43, 602.
- (21) Tomasi, J.; Mennucci, B.; Cammi, R. *Chem. Rev.* **2005**, 105, 2999.
- (22) Lochmann, L.; Trekoval, J. J. *Organomet. Chem.* **1987**, 326, 1.
- (23) (a) Sheldrick, G. M. In *SHELXL-97, Program for the Refinement of Crystal Structure from Diffraction Data*; University of Göttingen, Göttingen, Germany, 1997. (b) Sheldrick, G. *Acta Crystallogr., Sect. A* **2008**, A64, 112.
- (24) Frisch, M. J.; Trucks, G. W.; Schlegel, H. B.; Scuseria, G. E.; Robb, M. A.; Cheeseman, J. R.; Scalmani, G.; Barone, V.; Mennucci, B.; Petersson, G. A.; Nakatsuji, H.; Caricato, M.; Li, X.; Hratchian, H. P.; Izmaylov, A. F.; Bloino, J.; Zheng, G.; Sonnenberg, J. L.; Hada, M.; Ehara, M.; Toyota, K.; Fukuda, R.; Hasegawa, J.; Ishida, M.; Nakajima, T.; Honda, Y.; Kitao, O.; Nakai, H.; Vreven, T.; Montgomery, J. A., Jr.; Peralta, J. E.; Ogliaro, F.; Bearpark, M.; Heyd, J. J.; Brothers, E.; Kudin, K. N.; Staroverov, V. N.; Kobayashi, R.; Normand, J.; Raghavachari, E.; Rendell, A.; Burant, J. C.; Iyengar, S. S.; Tomasi, J.; Cossi, M.; Rega, N.; Millam, J. M.; Klene, M.; Knox, J. E.; Cross, J. B.; Bakken, V.; Adamo, C.; Jaramillo, J.; Gomperts, R.; Stratmann, R. E.; Yazyev, O.; Austin, A. J.; Cammi, R.; Pomelli, C.; Ochterski, J. W.; Martin, R. L.; Morokuma, K.; Zakrzewski, V. G.; Voth, G. A.; Salvador, P.; Dannenberg, J. J.; Dapprich, S.; Daniels, A. D.; Farkas, O.; Foresman, J. B.; Ortiz, J. V.; Cioslowski, J.; Fox, D. J. *Gaussian 09, Revision A.02*; Gaussian, Inc., Wallingford, CT, 2009.
- (25) Grimme, S. *J. Comput. Chem.* **2006**, 27, 1787.